Journal of Engineering and Development

www.jead.org
Vol. 20, No.1, January 2016
ISSN 1813-7822

FABRICATION AND CHARACTERIZATION OF PALLADIUM-DOPED ZINC OXIDE THIN FILMS AND ITS APPLICATION AS EXTENDED-GATE FIELD-EFFECT TRANSISTOR PH SENSOR

Dr.Raad HamdanThaher[1], Ghusoon Mohsin Ali[2], *Ali AzzamAbdullateef[3]

1) AssistProf., ElectricalEngineering Department, the Universityof Mustansiriayah, Baghdad, Iraq.
2) Lect., ElectricalEngineering Department, the Universityof Mustansiriayah, Baghdad, Iraq.
3) M.Sc. student, ElectricalEngineering Department, the Universityof Mustansiriayah, Baghdad, Iraq.

(Received:06/28/2015 ; Accepted:16/09/2015)

Abstract: This work presents the fabrication, characterization and performance analysis of Zinc Oxide (ZnO) and Palladium doped Zinc Oxide (Pd-ZnO) thin films based Extended-Gate Field-Effect Transistor (EGFET) pH sensor. The Pd-doped ZnO thin films with different molar concentrations (Pd = 0%, 2% and 4%) were deposited onto p-type Si<111> substrate by sol-gel method.The EGFET pH-sensor has been prepared by linking the fabricated sensing devices to the gate terminal of a commercial Metal Oxide Semiconductor Field-Effect Transistor (MOSFET CD4007UB). The fabricated sensing devices were immersed in buffer solutions with pH range of (pH 3 – pH 11).The pH sensing characteristics of ZnO and Pd-ZnO/silicon EGFET devices were studied using Semiconductor Characterization System (SCS-Keithley 4200). The undoped ZnO EGFET sensor exhibits current sensitivity and linearity of 46.17μA/pH and 97.81% with pH range of (pH 3 - pH 11) andthe current sensitivity and linearity of Pd-doped ZnO (with 4% molar concentration of Pd) EGFET sensor with pH range of (pH 5 - pH 11) are 44 μA/pH and 96.22%, respectively.

Keywords: *ZnO, Pd-ZnO, Sol-gel, EGFET, pH sensor.*

تصنيع و دراسة خصائص أغشية أوكسيد الزنك الرقيقة والمشوبة بالبلاديوم وتطبيقاتها في متحسس لتركيز الهيدروجين من نوع ترانزستور تأثير المجال ممدود البوابة

الخلاصة:يتناول هذا البحث تصنيع و توصيف و تحليل اداء متحسّسات تركيز الهيدروجين (pH sensor) من نوع ترانزستور تأثير المجال ممدود البوابة (EGFET) باستخدام أغشية اوكسيد الخارصين الرقيقة والمشوَّبة بالبلاديوم.تم ترسيب أغشية أوكسيد الخارصين المشوَّبة بتركيز مولي متنوع (Pd=0٪ و 2٪ و 4٪) على ركيزة من نوع سيليكون <111> باستخدام طريقة محلول-هلام (sol-gel). تم أعداد متحسّس تركيز الهيدروجين نوع ترانزستور تأثير المجال ممدود البوابة من خلال ربط أجهزة التحسّس المصنَّعة لمنفذ بوابة معدن-أوكسيد -شبه موصل ترانزستور تأثير-المجال (MOSFET CD4007UB). تم غَمُر أغشية التحسّس المصنَّعة في محاليل منظمة بمدى من الرقم الهيدروجيني (pH 5-pH 11).وقد تمت دراسة خصائص تحسّس أغشية أوكسيد الخارصين غير المشوَّبة والمشوَّبة بالبلاديومباستخدام منظومة توصيف أشباه الموصلات (Keithley-4200). أن أغشية أوكسيد الخارصين تبدي حساسية تيار وخطية للرقم الهيدروجيني بمقدار (46.17 μA/pH) و (97.81%) وبمدى (pH 3- pH 11) و أن أغشية أوكسيد الخارصين المشوَّبة بالبلاديوم (بمقدار 4٪ تركيز المولي من Pd) تبدي حساسية التيار وخطية بمقدار (44 μA/pH) و (96.22%) وبمدى (pH 5- pH 11).

*Corresponding Author ali.abdullateef27@yahoo.com

1. Introduction

In recent years, there is noteworthy interest in using pH-sensors based on Field Effect Transistor (FET) in biomedical applications such as human blood, urine, and saliva because the fabrication of pH-sensors is tending toward low cost, small size, disposable, and real-time measurement. The pH value is an important parameter in the environmental and medical detection. For example, a small change of pH value due to the wastewater from factories would threaten the living creatures inside the river or ocean. In addition, a small difference in pH value of the blood can wreck the balance of human body system. Many process industries also deal with pH measurements such as food industries, drugs and semiconductors.The structure of ion-sensitive field effect transistor (ISFET) was fabricated as an alternative to the fragile glass electrode by Bergveld in 1970 at the University of Twente [1].The main difference between ISFET and standard metal oxide-semiconductor field-effect transistor (MOSFET) is that there is no metal gate electrode in the former. Silicon dioxide (SiO_2) was the first sensitive membrane used in ISFET, which had several disadvantages such as unstable sensitivity and large drift.Many sensitive membranes were used as pH-sensing elements like Aluminum nitride (AlN) and Aluminum oxide (Al_2O_3) [2,3].The advantages of ISFET over conventional glass electrodes are miniaturization, high input impedance, low output impedance, easy to mass product and suitable for biosensor applications.

Extended Gate Field Effect Transistor (EGFET) was initially suggested as an alternative to ISFET in pH measurement by Van Der Spiegel and others in 1983 [4].The EGFET utilizes the same principle of operation of the ISFET.EGFET is a structure used to isolate MOSFET from the chemical environment. In 2000, Chi and others presented an improved structure of EGFET. The developed device consists of membrane sensitive to hydrogen ion (sensing part) and commercial MOSFET (CD4007UB) [5]. This structure has many advantages such as less sensitive to light, stable and flexible shape of the extended gate. Various materials were also used as the ion sensitive parts such as Tin oxide (SnO_2) and Titanium dioxide (TiO_2) [6,7]. Zinc oxide (ZnO) thin films are technologically important with wide range of electrical and optical properties [8], which make them suitable for many applications such as varistors, surface acoustic wave devices, transparent conducting electrodes, piezoelectric transducers, solar cells and gas sensors. ZnO is II-VI semiconductor materials with wide and direct band gap (~3.37eV) at room temperature, non-toxic material, cheap and good chemical and thermal stability. Zinc oxide was doped with various materials such as Aluminum, Gallium and Indium to modify specific properties[9,10,11]. In this work, the characterization and pH-sensing characteristics of palladium-doped ZnO thin films as pH-EGFET sensor were investigated.

2. Experimental Work

2.1. Thin Film Deposition

The cleaning of substrates isthefirst step to remove any contaminations and dirts. For deposition process, p-type silicon substrates Si<111>with thickness of (~500 μm)and resistivity 2–7 Ω.cm were used. The substrates were subjected to cleaning process in ultrasonic bath for five minutes using trichloroethylene ($CICH.CCL_2$), immersed in acetone for one minute, cleaned in a solution of 40mL of Sulphuric acid (H_2SO_4) and 60 mL of hydrogen peroxide (H_2O_2), and cleaned in de-ionized water(resistivity = 18 MΩ.cm) [12].

For un-doped ZnO film, 1.75 gram powder solute quantity of Zinc acetate dihydrate ($Zn(CH_3COO)_2,2H_2O$) was dissolved in 20 mL of isopropanol ($(CH_3)_2CHOH$) and 0.8 gram Diethanolamine ($C_4H_{11}NO_2$) at room temperature to synthesize 0.4 mole/Liter concentration of aqueous precursor solution of ZnO. For Pd-doped ZnO solutions, 0.02 (2%) and 0.04 (4%) mole/liter concentrations of aqueous precursor solutions of Palladium (II) nitrate dehydrate ($2NO_3.Pd.2H_2O$) were prepared by dissolving powder quantity of 0.11 and 0.21 grams of Palladium (II) nitrate dehydrate (the solute) in solutions of 20mL isopropanol (the solvent), 1.75 gram of Zinc acetate dehydrate and the desired amount of Diethanolamine, respectively. The molar concentration of Zinc acetate dihydrates was 0.4 mole/Liter. The resultant solutions were mixed at room temperature by a magnetic stirrer for 1 h to obtain clear and homogeneous solutions[13].

ZnO and Pd-dopedZnO films were prepared by spin coating the precursor solutions on the substrates for 50 second at a speed of 4,000 rpm. This step was followed by preheating the coated substrates at 100 $^{\circ}$C for 10 minutes by a hot plate device. The spin coater and hot plate devices (model: CHEMAT TECHNOLOGY, KW-4A).The coating and preheating steps were repeated for three times. Then, the deposited films were annealed at 450 $^{\circ}$C for 1 hour by conventional thermal annealing device (Model: MTI, KSL-1100X).

2.2. Surface Morphology and Crystal Structure

In this study, the surface morphology of Pd-doped zinc oxide films deposited onto the Silicon substrates using sol-gel synthesis was imaged by a field emission scanning electron microscope (FE-SEM) (model: FE-SEM, Tescan Vega III) and atomic force microscopy (AFM) (model: NT-MDT, SPM Ntegra). The crystal structure of deposited films was examined by the X-ray diffractometer device (model: Lab X XRD-6000, Shimadzu)with Cu Kα radiation, voltage 40 kV, current 30 mA.

2.3. Electrical Properties

Hall Effect measurement system (model: Ecopia, HMS-3000) was used to measure the electrical characteristics of thin films with magnetic field and constant current value of (0.55 Tesla and 100μAmpere) respectively. Van der Pauw square geometry sample was used with 1.5 cm length of sides and four aluminum triangular contacts at the corners.

2.4. Palladium Comb-Like Electrode

A ten finger metal mask was used to thermally evaporate the Palladium comb like electrodes on the fabricated ZnO samples. The deposited fingers were designed to have a width of 0.5 mm, a length of 16 mm, and spacing of 2 mm between the mask fingers. This design has proven to be reliable throughout our work. Then, the sensing filmswere bound to a metal wire with silver paste (electrical contact). Then, the wire-bond region was encapsulated by epoxy resin to prevent electrical contact with the electrolyte and avoid leakage current during measurements. The sensing area was determined at 2.5 cm× 2.5 cm by epoxy resin. The cross section of the pH sensing electrode is shown in Fig.1.

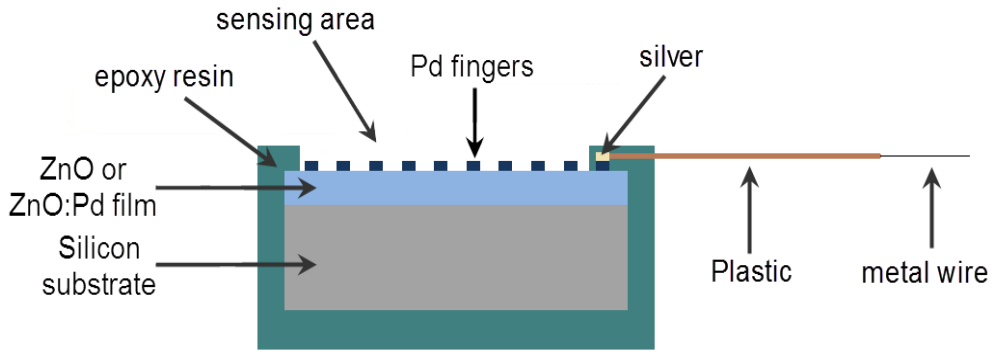

Figure 1: Cross section of the sensing electrode of EGFET.

2.5 Current-Voltage Measurement System of EGFET pH Sensor

The (I-V) measurement system is shown in Fig. 2. In this work, commercial MOSFET (model: CD4007UB, RCA Solid State Division) was used. This device has good characteristics and also commercially available. The gate terminal of n-channel transistor was connected to the sensing structurewhile the drain and source terminals were connected to Semiconductor Characterization System (model: SCS 4200, Keithley Instruments, Inc.) via a bread board. The reference electrode was Ag/AgCl electrode (model: Digi-Ivy, Inc.), providing a bias voltage on the sensing electrode. To measure the sensing performance of the fabricated pH sensor, the sensing unit and the Ag/AgCl reference electrode were immersed in a beaker containing electrolyte buffer solution for 15 seconds before measuring, and the distance between the reference electrode and sensing unit was kept at about 1 cm. After each measurement, the sensing gate was rinsed in de-ionized water for 15 seconds before conducting another measurement in a new buffer solution in order to remove any residual chemical compounds. All measurements were achieved at room temperature.

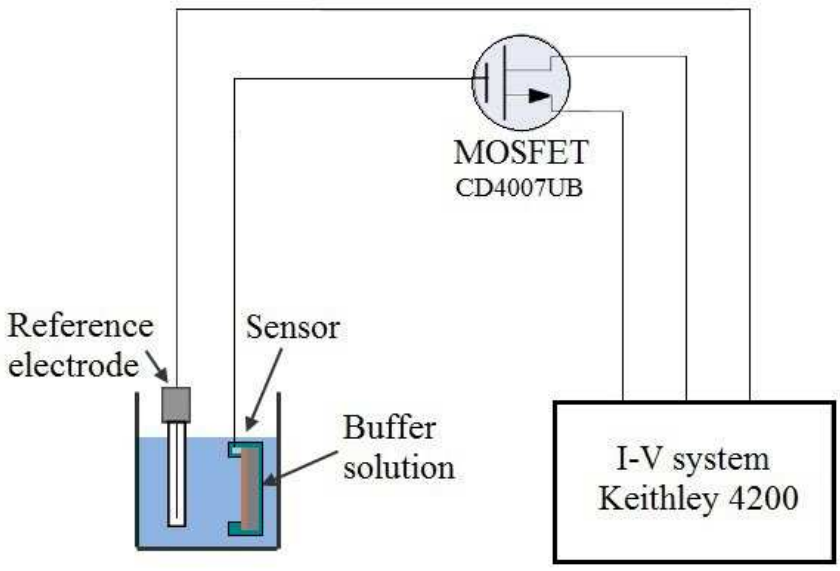

Figure 2: (I-V) measurement system of EGFET.

3. Results and Discussions

3.1 Surface Morphology of films

The influence of Pd doping on the surface morphology of ZnO and (ZnO:Pd) films is shown in Fig.3. The AFM and SEM topographical images show that the ZnO and Pd-doped ZnO films have homogeneous and uniform surfaces without any cracks. The scanned area is too small compared to the whole thin film area. But, it still provides a positive hint about homogeneity and absences of surface cracks. From AFM results, thegrain sizes were 36.1 nm, 37.3 nm, and 41.6 nm for undoped, 2%, and 4% Pd-doped ZnO thin films, respectively.

The clustering of the grains is clearly observed in Pd-doped ZnO films.However, there is no significant difference in grain size between undoped and 2% Pd-doped ZnO films. The SEM topographical nanograph with 100kx magnification inFig.3(a)shows that the undoped ZnO film consists of densely packed nanoparticlesas in AFM image. In 2% Pd-doped ZnO film Fig. 3(b), tiny grains were merged to larger one; result in a small increase in grain sizeand this is clearly observed in AFM image. Fig. 3(c) proves that the 4% Pd-doped ZnO thin film consists of agglomerations like clusters result in an increase in grain size and this in good agreement withAFM image. From AFM test, Root mean square (RMS) value of surface roughness were 2.553, 1.817 and 1.625 nm for undoped ZnO, 2%, and 4% Pd-doped ZnO thin films, respectively. The small values of surface roughness indicate the formation of granular nanostructures in ZnO and ZnO:Pd films. The decrement in surface roughness of the deposited films is clearly observed in SEM images.

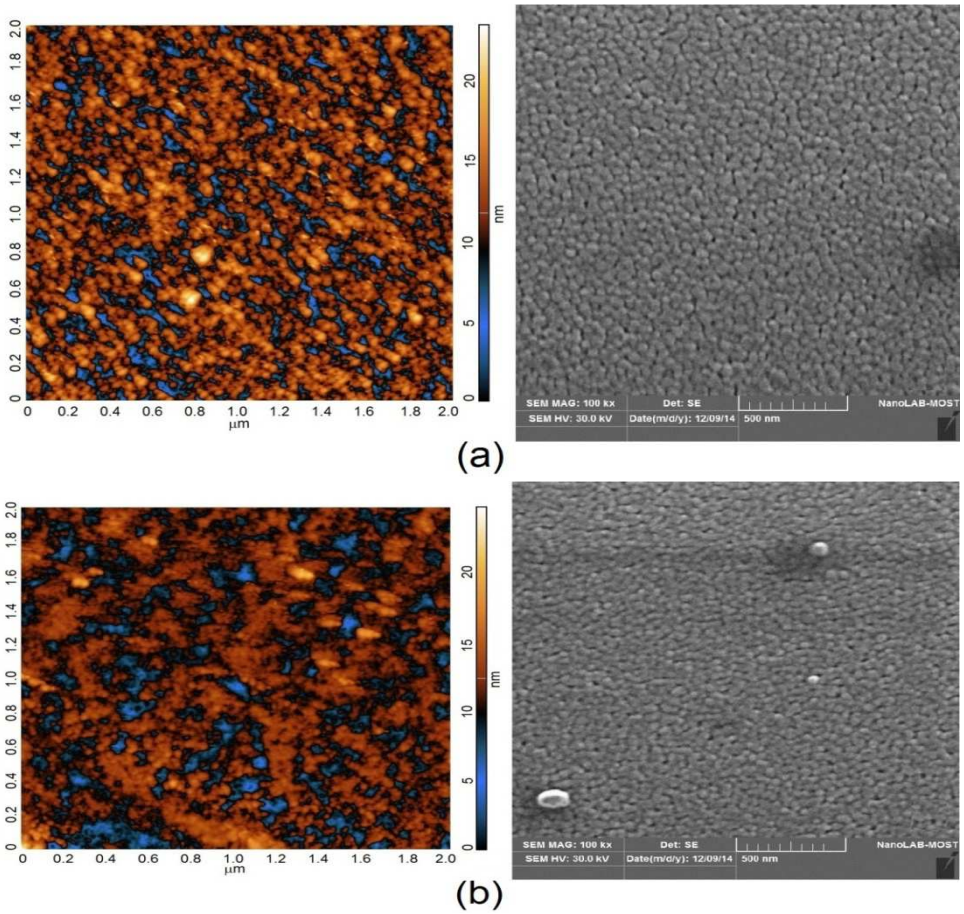

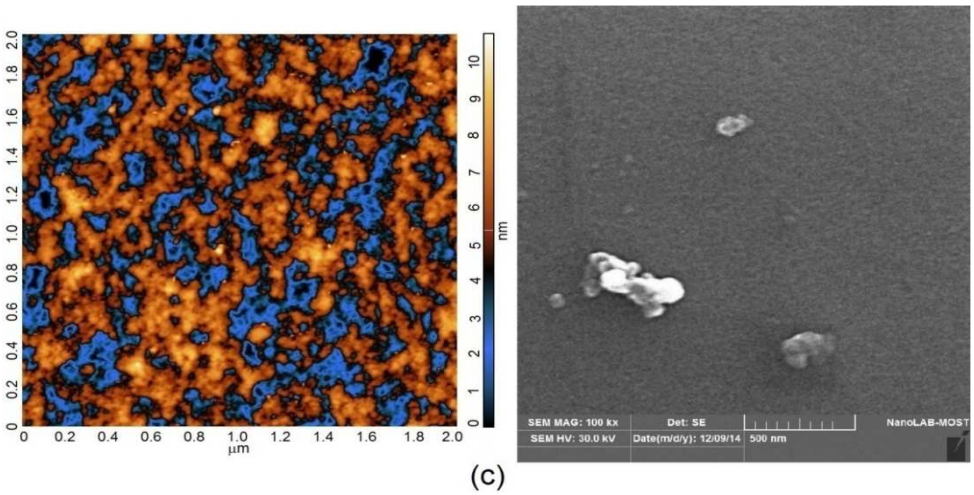

Figure 3: AFM and SEM images of (a) undoped ZnO film (b) 2% Pd-doped ZnO film (c) 4% Pd-doped ZnO film.

The thickness of the deposited films was estimated using the SEM cross-section images of the prepared structures as shown in Fig. 4. The thickness of the undoped ZnO, 2%, and 4% Pd-doped ZnO was about 110 nm, 600 nm and 610 nm, respectively. The diminution in surface roughness of the prepared films with increasing dopant concentration was clearly observed by SEM cross-section images.

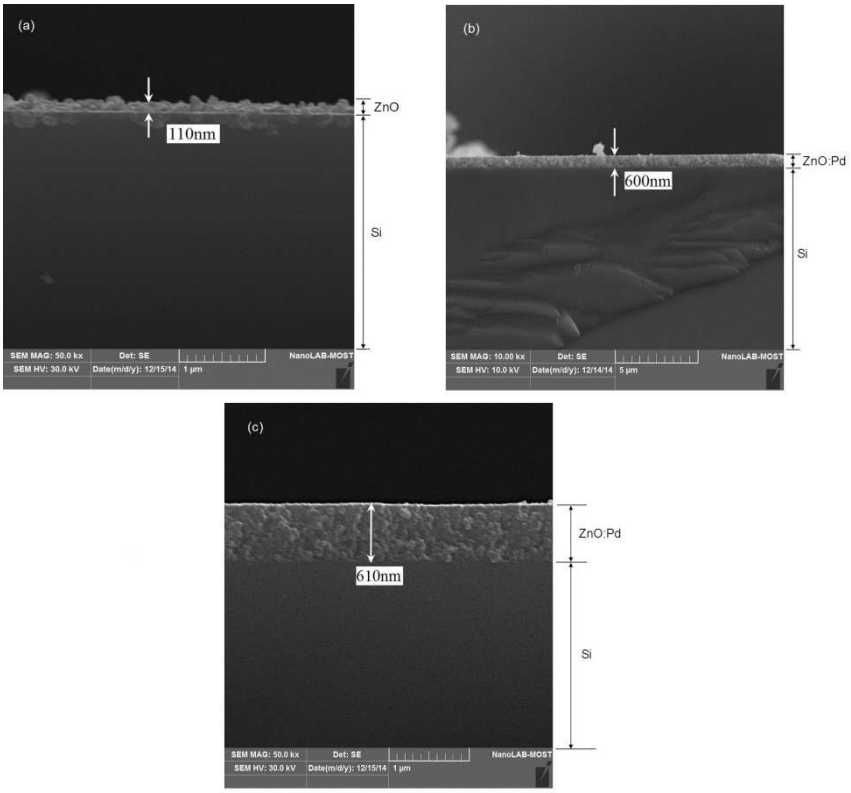

Figure 4: SEM cross-sections of (a) ZnO/Si, (b) ZnO:Pd/Si with 2% Pd doped and (c) ZnO:Pd/Si with 4% Pd doped structures.

3.2 Crystal Structure

The XRD patterns of the prepared films are obtained by X-ray diffractometer with 2θ starting from 20° to 50° as shown in Fig.5. The diffraction peaks of all films are fairly

matching with the hexagonal wurtzite ZnO structure (JCPDS card no. 36-1451). There are no peaks corresponding to the dopant (Pd) regardless of the dopant concentration, which may be due to the low amount of Pd doping. In undoped ZnO thin film, four peaks that correspond to the (100), (002), (101), and (102) directions of the hexagonal ZnO crystal structure are appeared at 31.82°, 34.45°, 36.32°, and 47.62° respectively with no presence of dominant peak. The c-axis lattice constant was calculated as5.202Å.

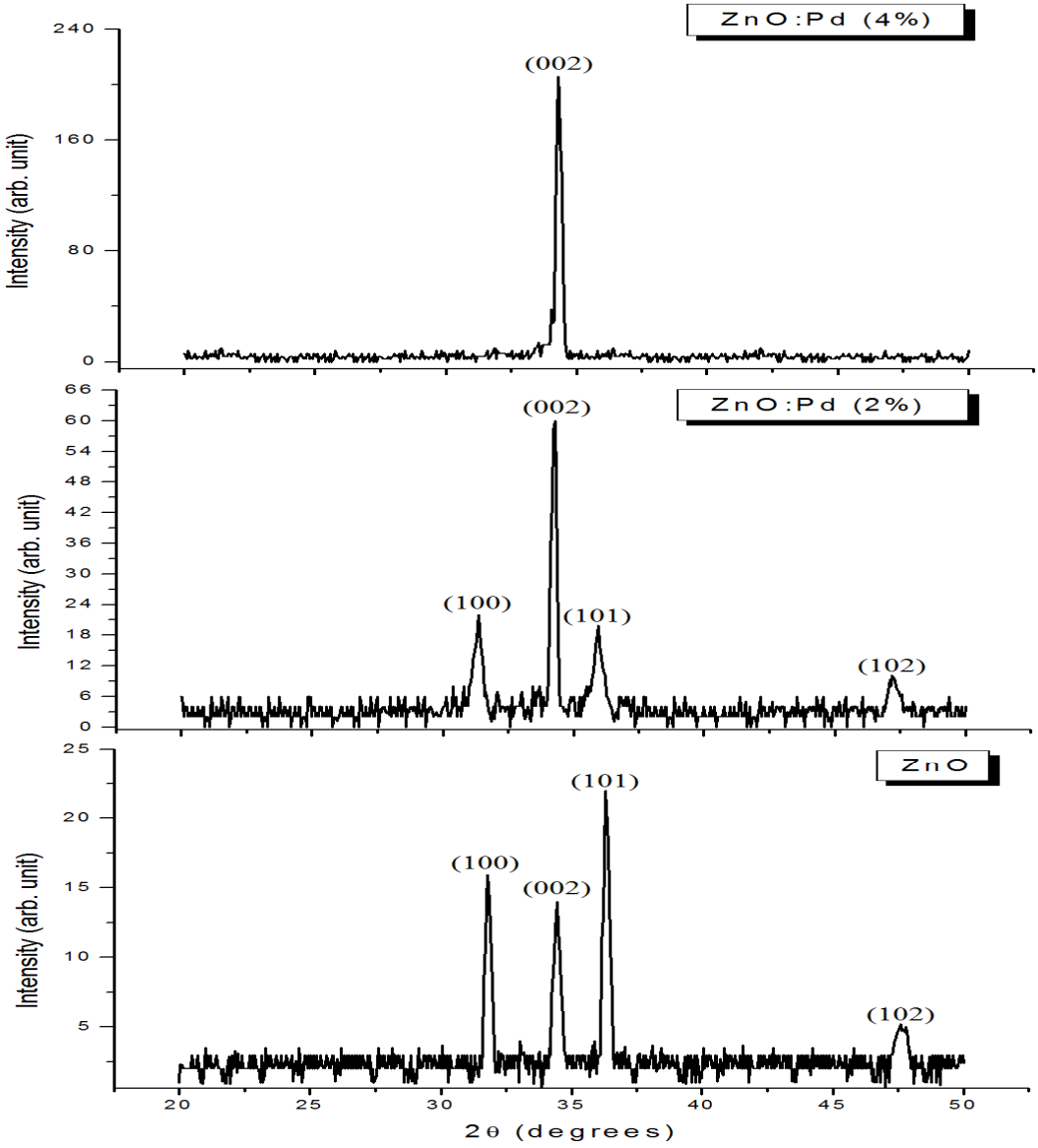

Figure 5: The XRD spectra of undoped and Pd-doped ZnO thin films.

In 2% Pd-doped ZnO thin film, one sharp peak at 34.30° and three small peaks at 31.42°, 35.93, and 47.22° are observed corresponding to the crystal planes (002), (100), (101), and (102), respectively. The ratio of the intensities of the peaks (002) to (100), i.e., I_{002}/I_{100}, is about 3 suggesting preferential growth along the c-axis, which indicated by the plane (002).The c-axis lattice constant was calculated as5.224Å. In 4% Pd-doped ZnO thin film, the only diffraction peak is the ZnO (002) peaks located at 34.28° whereas the secondary peaks corresponding to the crystal planes (100) and (101) are negligibly small. This film has enough

preferred orientation (002) crystal plane along the c-axis, which indicated that the film is polycrystalline with a hexagonal wurzite structure [14].

The c-axis lattice constant was calculated as5.226Å. In Pd-doped ZnO films, deviation in peak positions to lower angles is clearly observed and the corresponding d-spacing becomes larger than standard d-spacing($d_{measured}>d_{standard}$) due to the effect of the uniform tensile (positive) strain [15]. Lattice strain is arising from crystal imperfections, such as lattice dislocations. One of the sources of strain is the grain boundary (GB) [16]. Grain boundaries are defects in the crystal structure, and lead to decrease the electrical properties of the film. Therefore, the mobility of charge carriers was decreased in this film, as illustrated in Hall-effect measurement later. The diffracted intensity increases by increasing the dopant concentration due to increasing the size of ZnO particles [17]. It's observed that the lattice constants (c) increases with the dopant concentration. This variation in lattice constants preliminarily denotes that Pd^{2+} ions substitute of Zn^{2+} ions in the ZnO lattice because of the larger ionic radius of Pd^{2+} ion (0.086 nm) than ionic radius of Zn^{2+} ion (0.074 nm) [18].

3.3 Hall Effect measurement of films

The measured electrical properties of the ZnO and ZnO:Pd sensing films like carrier concentration, resistivity, mobility, and semiconducting type are summarized in Table 1. Hall-effect measurements indicate that ZnO and ZnO:Pd films are n-type materials. The observed diminution in mobility of 2% Pd-doped ZnO film may be due to the presence of the grain boundaries, resulting in the scattering and trapping of the charge carriers at grain boundaries, as previously illustrated in XRD results. Therefore, when the grain boundary density decreased the mobility increased. The increasing in the mobility of 4% Pd-doped ZnO film as compare with 2% doping concentration film may be attributed to the increasing in the grain size and improving in crystallinity with doping. Hall measurements indicate that there is no significant change in carrier concentration of deposited films regardless of the doping concentrations, resulting in no considerable change in the resistivity of the Pd-doped ZnO films, which can be attributed to the low amount of dopant material in the synthesized films [12].

Table 1Electrical characteristics of the sensing films by hall-effect.

Sensing film	*ZnO*	*ZnO:Pd (2%)*	*ZnO:Pd (4%)*
Current(μA)	100	100	100
Magnetic field (T)	0.55	0.55	0.55
Mobility (cm^2/Vs)	114.1	96.9	112.6
Resistivity (Ω.cm)	29.6×10^{-2}	33.5×10^{-2}	47.1×10^{-2}
Carrier concentration (cm^{-3})	1.85×10^{17}	1.92×10^{17}	1.18×10^{17}

3.4 Sensing Performance of ZnO and Pd-doped ZnO Based EGFET pH Sensor

To investigate the sensing performance of the ZnO and Pd-doped ZnOEGFET pH sensors in solutions of various pH values, The output characteristics (drain current versus drain source voltage, I_{DS}–V_{DS}) of the undoped ZnO, 2%, and 4% Pd-doped ZnO sensing films with (V_{GS} =

4 V and V_{DS} varied from 0 to 5 V) are measured as shown in Fig.6, 7 and 8, respectively. These curves are plotted by MATLAB software. From these curves, it is observed that the drain-source current (I_{DS}) decreased with the increase of the pH value. This behavior can be explained as follow; at high pH values, low amount of hydrogen ions presented in the solution according to the definition of pH:

$$pH = -\log_{10}(H^+) \quad (1)$$

This means that there are small amount of hydrogen ions adsorbed (accumulated) onto the surface of the sensing membrane, which in turn leads to small surface potential voltage (ψ) on the sensing membrane and large threshold voltage $V_{T(EGFET)}$ as expressed:

$$V_{T\,(EGFET)} = \underbrace{V_{T\,(MOSFET)} + \Delta\varphi^{lj} + E_{REF} + \chi^{sol}}_{\text{Constant}} \underbrace{- \psi}_{\text{Variable}} \quad (2)$$

where $V_{T(MOSFET)}$ is the threshold voltage of the MOSFET, $\Delta\varphi^{lj}$ is the liquid-junction potential difference between the reference electrode and the solution, E_{REF} is reference electrode potential, and χ^{sol} is the surface dipole potential of the electrolyte, which is a constant [19].The large threshold voltage $V_{T(EGFET)}$, in turn, leads to the small drain-source current (I_{DS}) of the EGFET sensor as expressed inthe I-V characteristics for EGFET sensor:

$$I_D = K_n (V_{GS} - V_{T(EGFET)})^2 \quad (3)$$

Where I_D is the drain current and K_n is the conduction parameter for the n-channel enhancement MOSFET[20].

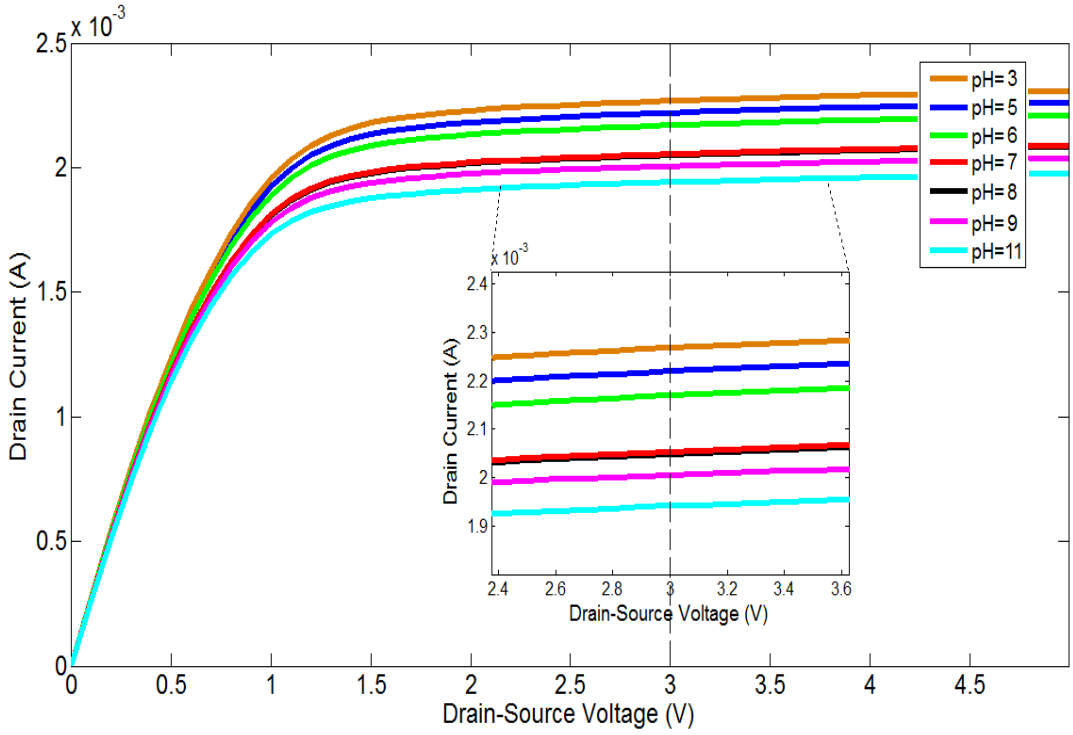

Figure 6: output characteristics (I_{DS}–V_{DS}) of ZnO EGFET sensor in the saturation region.

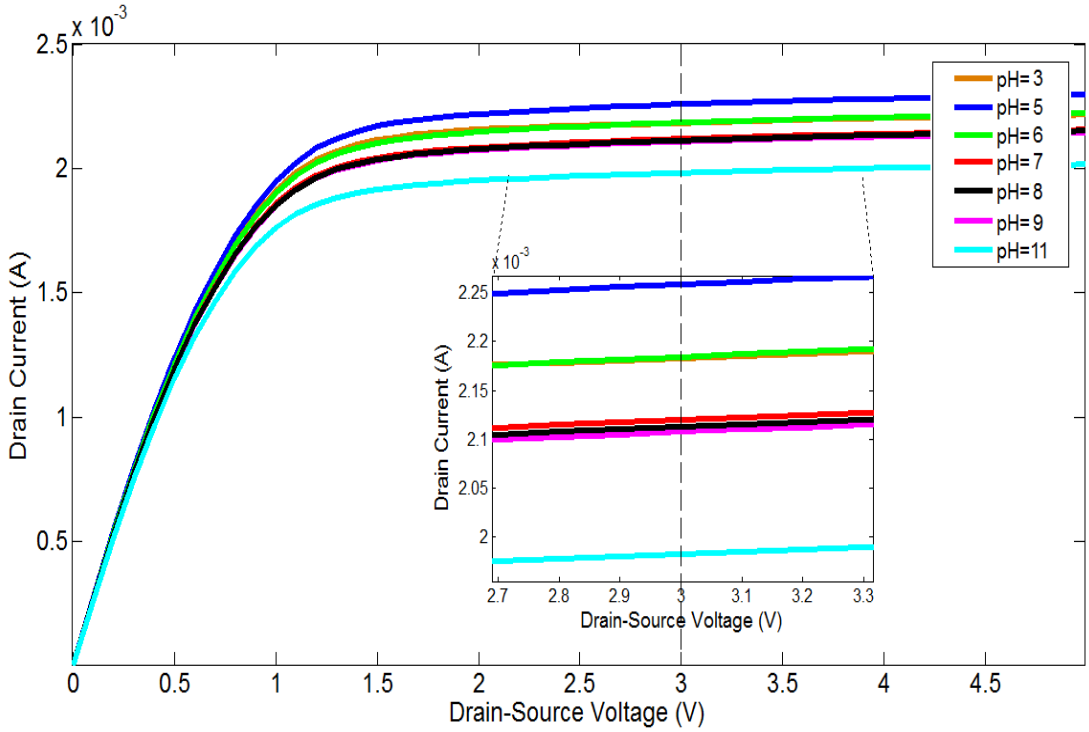

Figure 7: output characteristics (I_{DS}–V_{DS}) of 2% Pd-dopedZnO EGFET sensor in the saturation region.

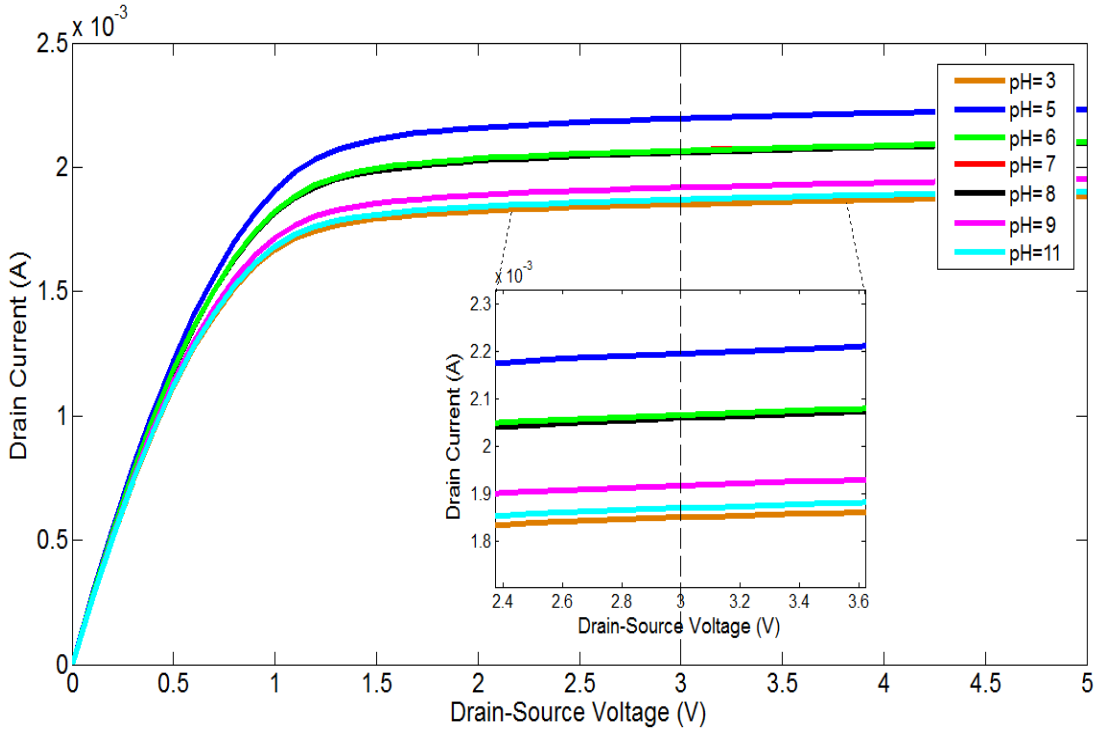

Figure 8: output characteristics (I_{DS}–V_{DS}) of 4% Pd-dopedZnO EGFET sensor in the saturation region.

In each curve, the drain-source voltage (V_{DS}) is fixed at 3 V as reference value so that the MOSFET device (CD4007UB) can be operated in the saturation region. From this value, a line parallel to the Y axis is drawn. The intersection of this line with (I-V) curve of each pH value gives seven points with coordinate (V_{DS}=3 V, $I_{DS_{pH}}$). From these points, the I_{DS} and pH values with coordinate (pH, I_{DS}) are taken and plotted in order to calculate the current sensitivity and

linearity. Sensitivity is one of the important parameters for a sensor device and the definition of the current sensitivity is that the dependence of the measured drain-source current (I_{DS}) on the pH value(current sensitivity = $\Delta I_{DS}/\Delta pH$).Sensitivity and linearity can be calculated by linear fitting between I_{DS} and pH values using MATLAB software and Origin Pro 6.0 software, respectively. Hence the sensitivity is the slope of the linear fit line and the linearity is defined as the correlation coefficient of the linear fit. pH current sensitivity curves of undoped, 2%, and 4% Pd-doped ZnO sensing films are shown in Fig.9, 10 and 11 respectively.

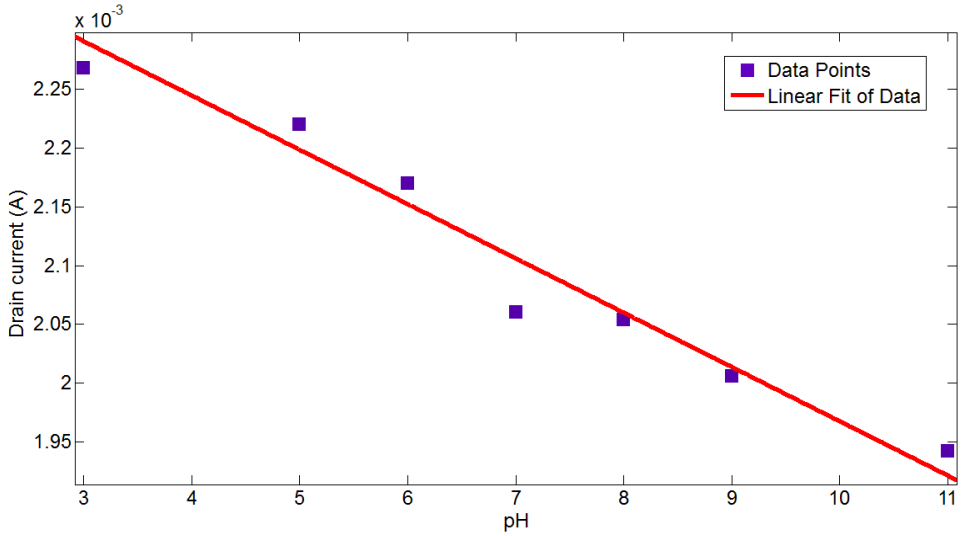

Figure 9: pH currentsensitivity of undoped-ZnO EGFET in the saturation region.

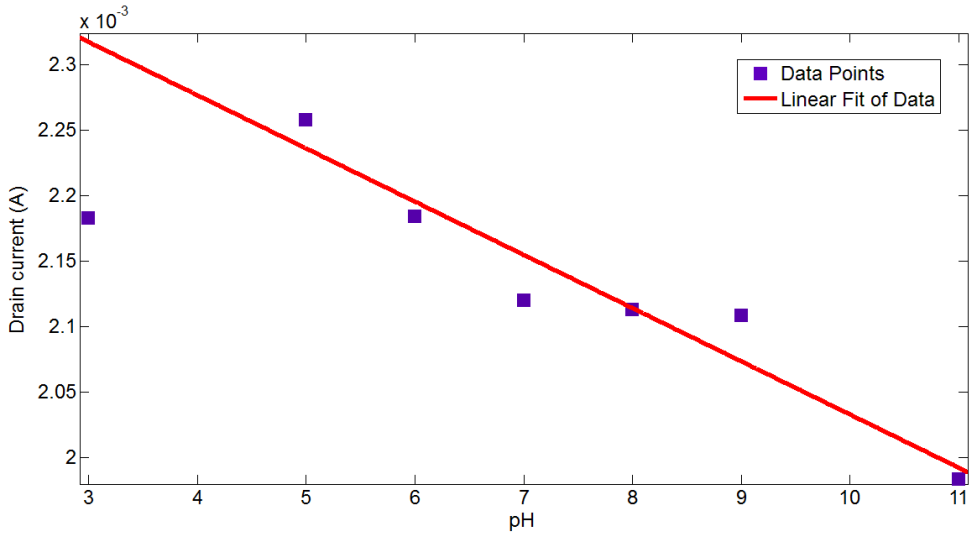

Figure 10: pH currentsensitivity of 2% Pd-doped ZnO EGFET in the saturation region.

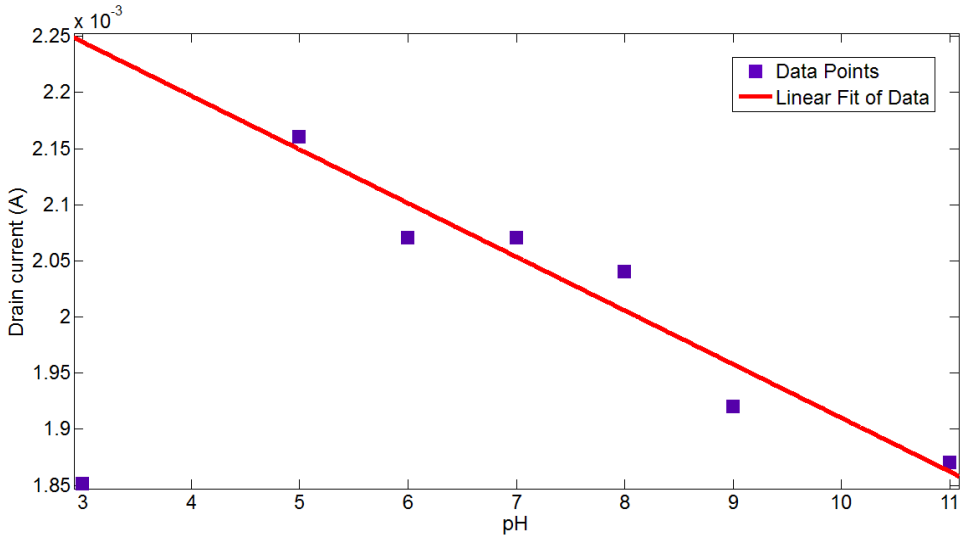

Figure 11: pH currentsensitivity of 4% Pd-dopedZnO EGFET in the saturationregion.

According to the linear fit, the current sensitivity and linearity of undoped ZnO EGFET device in the range of pH 3 to 11 are 46.17 μA/pH and 0.9781 (or 97.8%), respectively. The current sensitivity and linearity of 2%Pd-doped ZnO EGFET device in the range of pH 5 to 11 are 40.7 μA/pH and 0.9621 (or 96.21%), respectively. The current sensitivity and linearity of 4%Pd-doped ZnO EGFET device in the range of pH 5 to 11 are 44 μA/pH and 0.9622 (or 96.22%), respectively. The transfer characteristics (drain current versus gate-source voltage, I_{DS}–V_{GS}) of the 0% (undoped), 2%, and 4% Pd-doped ZnO sensing films in the linear region (V_{DS} = 0.2 V) and V_{GS} varied from 0 to 4 V were mentioned in reference [21].

The voltage sensitivity (voltage sensitivity = $\Delta V_{GS}/\Delta pH = \Delta V_T/\Delta pH$) was derived fromthe transfer characteristics under constant current(300 μA). The voltage sensitivity and linearity of ZnO EGFET device in the range of pH 3 to 11 are 31.5 mV/pH and 0.9809 (or 98.1%), respectively. This result is not far away from that in ref. [22]. The voltage sensitivity and linearity of 2% Pd-doped ZnO EGFET device in the range of pH 5 to 11 are 24.41 mV/pH and 0.9774 (or 97.74%), respectively. The voltage sensitivity and linearity of 4% Pd-dopedZnO EGFET device in the range of pH 5 to 11 are 27.86 mV/pH and 0.9785 (or 97.85%), respectively[21].

4. Conclusions

In this work, ZnO and Pd-doped ZnO thin films were developedas sensing devices of EGFET pH sensor. pH sensing characteristics of ZnO and Pd-ZnO thin films as sensing electrodes for EGFET pH sensor device were investigated in buffer solutions with range of pH (3 – 11). The ZnO pH-EGFET sensors present the optimum pH-sensing characteristics in this work (i.e., the higher voltage sensitivity of 31.5 mV/pH, the larger linearity of 0.9809 (or 98.1%) in linear region, the higher current sensitivity of 46.17 μA/pH, the larger linearity of 0.9781 (or 97.8%) in saturation region and the wider sensing range of (pH 3 – pH 11), which may be attributed to the vertically well-aligned nanoparticles, high surface roughness, large amount of surface sites for H^+ ion adsorption, less structural defects, and high carrier mobility. In Pd-doped ZnO films, pH sensing characteristics of Pd-doped ZnO film with Pd dosage of 4% is better than 2% Pd-doped ZnO film. This improvement in sensing properties can be

attributed to the increasing in grain size due to the clustering of grains and improvement in crystallinity with doping concentration. This can cause a decrease in grain boundary scattering and an increase in carrier mobility. As observed, Pd-doped ZnO films cannot distinguish pH value of 3. This behavior refers to that the doped sensing films by sol-gel method do not work for the whole pH range because the doped ZnO films have less hydroxyl-bonding sites for adsorption of H^+ ions than ZnO films at its surfaces.At the same time, the linearity and pH voltage sensitivity of the ZnO based EGFET sensor are also better than Pd-doped ZnO based EGFET sensor regardless of dopant concentration. This agrees with the above stated reasons.

Acknowledgement

The authors acknowledge the ministry of science and technology specially the staff of solar cell preparation laboratory and solar cell evaluation laboratory, for collaboration and allowance to use their laboratory**.** In addition, the authors are also grateful to Dr. Falah I. Mustafa the head of solar energy research center.

5. References

1. B. P. Bergveld (1970).*"Development of an ion sensitive solid-state device for neurophysiological measurement"*, IEEE Transactions on Biomedical Engineering, Vol. 17, No. 1, pp. 70–71.
2. J. L. Chiang, S. S. Jan, Y. C. Chen and J. C. Chou(2000).*"Sensing characteristics of ISFET based on AlN thin film"*, Proc. Of SPIE–The International Symposium on Optoelectronic Materials and Devices II, Taipei, Taiwan, Vol. 4078, pp. 689-696.
3. L. Bousse, H. V. Den Vlekkert and N. F. de Rooij (1990).*"Hysteresis in Al_2O_3 gate ISFETs"*, Sensors and Actuators B,Vol. 2, pp. 103-110.
4. J. van der spiegel, I. Lauks, P. Chan, and D. Babic (1983).*"The extended gate chemically sensitive field effect transistor as multi-species microprobe"*, Sensors and Actuators, Vol. 4, pp. 291–298.
5. L.L. Chi, J.C. Chou, W.Y. Chung, T.P. Sun, and S.K. Hsiung (2000).*"Study on extended gate field effect transistor with tin oxide sensing membrane"*, Materials Chemistry and PhysicsVol. 63 pp. 19–23.
6. L.T. Yin, J.C. Chou, W.Y. Chung, T.P. Sun, and S.K. Hsiung (2000).*"Separate structure extended gate H-ion sensitive field effect transistor on a glass substrate"*, Sensors and Actuators B Vol. 71 pp. 106-111.
7. P.C. Yao, J.L. Chiang , and M.C. Lee (2014).*"Application of sol-gel TiO_2 film for an extended-gate H ion-sensitive field-effect transistor"*, Solid State Sciences Vol. 28, pp. 47-54.
8. A. Janotti and Chris G. Van de Walle (2009).*"Fundamentals of zinc oxide as a semiconductor"*, Rep. Prog. Phys., 72, pp. 126501–126529.
9. J. Oda, J. Nomoto, T. Miyata and T. Minami (2010).*"Improvements of spatial resistivity distribution in transparent conducting Al-doped ZnO thin films deposited by DC magnetron sputtering"*, Thin Solid Films, Vol. 518, pp.2984-2987.

10. W. T. Yen, J. H. Ke, H. J. Wang, Y. C. Lin, and J. L. Chiang (2009).*"Influences on optoelectronic properties of damp heat stability of AZO and GZO for thin film solar cells"*, Advanced Materials Research: Multi-Functional Materials and Structures II, pp. 79 - 82.
11. H. C. Pan, M. H. Shiao, C. Y. Su and C. N. Hsiao (2005).*"Influence of sputtering parameter on the optical and electrical properties of zinc doped indium oxide thin films"*, Journal of Vacuum science technology A, Vol. 23, pp. 1187-1191.
12. G. M. Ali, J. C. Moore, A. K. Kadhim and C. Thompson (2014).*"Electrical and optical effects of Pd microplates embedded in ZnO thin film based MSM UV photodetectors: A comparative study"*, Sensors and Actuators A Vol. 209, pp. 16– 23.
13. J.b.Zhong, J. Li, X. He, J. Zeng, Y. Lu, W. Hu, and K. Lin (2012).*"Improved photocatalytic performance of Pd-doped ZnO"*,Curr. Appl. Phys., Vol. 12.
14. J. L. Chiang and C. Y. Kuo (2013).*"Study on the Characterizations and Applications of the pH-Sensor with GZO/Glass Extended-Gate FET"*, IEEE 5th International Nanoelectronics Conference (INEC).
15. A. Khorsand Zak, W.H. Abd. Majid, M.E. Abrishami, and RaminYousefi (2011).*"X-ray analysis of ZnO nanoparticles by Williamson-Hall and size-strain plot methods"*, Solid State Sciences Vol. 13 pp. 251-256.
16. J. Zhang, Y. Zhang, K.W. Xu, V. Ji (2006).*"General compliance transformation relation and applications for anisotropic hexagonal metals"*, Solid State Communications Vol. 139, 87.
17. B. Sankara Reddy, S. Venkatramana Reddy, N. Koteeswara Reddy and J. Pramoda Kumari (2013).*"Synthesis, Structural, Optical Properties and Antibacterial activity of co doped (Ag, Co) ZnO Nanoparticles"*, Research Journal of Material Sciences, Vol. 1(1), p.p. 11-20, February.
18. J. Kaur1, P. Kumar, T. S. Sathiaraj and R. Thangaraj (2013).*"Structural, optical and fluorescence properties of wet chemically synthesized ZnO:Pd^{2+} nanocrystals"*, a Springer Open Access International Nano Letters, 3:4.
19. R. E. G. van Hal, J. C. T. Eijkel, and P. Bergveld (1996).*"A general model to describe the electrostatic potential at electrolyte oxide interfaces"*, Advances in Colloid and Interface Science, Vol. 69, pp. 31–62.
20. Jacob Millman and Arvin Grabel(1988).*"Microelectronics"*, Second Edition, McGraw-Hill.
21. Ghusoon M. Ali, and Ra'ad H. Dhaher, and Ali A. Abdullateef (1988).*"pH Sensing Characteristics of EGFET based on Pd-Doped ZnO Thin Films Synthesized by Sol-gel method"*, 2015 IEEE the Third International Conference on Technological Advances in Electrical, Electronics and Computer Engineering (TAEECE2015).
22. P. D. Batista and M. Mulato(2005).*"ZnO extended-gate field-effect transistors as pH sensors"*, Applied Physics Letters, Vol. 87, No.14, Article ID 143508.